USSR Report

ENGINEERING AND EQUIPMENT

NOTE

JPRS publications contain information primarily from foreign newspapers, periodicals and books, but also from news agency transmissions and broadcasts. Materials from foreign-language sources are translated; those from English-language sources are transcribed or reprinted, with the original phrasing and other characteristics retained.

Headlines, editorial reports, and material enclosed in brackets [] are supplied by JPRS. Processing indicators such as [Text] or [Excerpt] in the first line of each item, or following the last line of a brief, indicate how the original information was processed. Where no processing indicator is given, the information was summarized or extracted.

Unfamiliar names rendered phonetically or transliterated are enclosed in parentheses. Words or names preceded by a question mark and enclosed in parentheses were not clear in the original but have been supplied as appropriate in context. Other unattributed parenthetical notes within the body of an item originate with the source. Times within items are as given by source.

The contents of this publication in no way represent the policies, views or attitudes of the U.S. Government.

PROCUREMENT OF PUBLICATIONS

JPRS publications may be ordered from the National Technical Information Service (NTIS), Springfield, Virginia 22161. In ordering, it is recommended that the JPRS number, title, date and author, if applicable, of publication be cited.

Current JPRS publications are announced in Government Reports Announcements issued semimonthly by the NTIS, and are listed in the Monthly Catalog of U.S. Government Publications issued by the Superintendent of Documents, U.S. Government Printing Office, Washington, D.C. 20402.

Correspondence pertaining to matters other than procurement may be addressed to Joint Publications Research Service, 1000 North Glebe Road, Arlington, Virginia 22201.

USSR REPORT

ENGINEERING AND EQUIPMENT

CONTENTS

TURBINE AND ENGINE DESIGN

NAVIGATION AND GUIDANCE SYSTEMS

FLUID MECHANICS

AERONAUTICAL AND SPACE

SELECTION OF EFFECTIVE ARRANGEMENT OF HEAVY UNDERCARRIAGE SYSTEMS FOR USE WITH
CONCRETE RUNWAYS

AVDYUKHINA, T. M.

[Abstract] A study is made of various arrangements of heavy aircraft land-
ing gear for use on concrete runways. Running gear mass is used as the
optimization criterion. It is found that as the number of wheels increases
there is no stable tendency toward decreasing landing gear mass. In the
200-250 t takeoff weight range as the number of wheels varies from 8 to
24 for 4-truck landing gear, 12 to 36 for 6-truck landing gear, landing gear
mass does not decrease smoothly. The optical number of wheels on aircraft
with a takeoff weight of 200 t is found to be 12 for both 4 and 6 truck
landing gear. Figures 4, references 5 Russian.
[124-6508]

DURABILITY CALCULATION OF WING PANEL ELEMENT

KIRILLOV, A. V. and MOSTOVOY, A. S., Kuybyshev Aviation Institute

[Abstract] About 85% of all fatigue fractures in aircraft structural com-
ponents occur in joinings. Thus it is important to be able to predict dura-
bility of these components. The authors consider a method of determining
the durability of the joint of a wing panel element: a stringer loaded by
cyclic asymmetric tension. The stringer is demountable, and has one central
and two lateral fish plates at the connection points. All components of
the joint were made of D16T alloy. The proposed method of determining dura-
bility is based on the linear-discrete hypothesis of accumulation of fatigue

damage. A flowchart is given of a program for simulation of the process of fatigue fracture on the M4030 computer. The results of calculation show satisfactory agreement with experimental data from a plant of the Ministry of the Aviation Industry. Figures 7, references 8 Russian.
[144-6610]

PLANNING OF AIR CUSHION TRANSPORT VEHICLES

BADYAGIN, A. A., BAYDIN, A. I. and SHCHERBAKOV, B. S.

[Abstract] A study is made of the design of an air cushion vehicle in which
bypass engines are used to provide the air for the air cushion and the
reaction force to move the vehicle. When the engines are first started, all
of the air from the outer path is used to create the air cushion. As the
vehicle accelerates, less of the air from this path is used to support the
cushion, and finally at full speed all of the air is used to move the
vehicle, with aerodynamic forces maintaining the cushion. It is concluded
that there is an optimal ratio of air flow through the two paths in the
engine. The optimal length of the acceleration run increases with in-
creasing mass of the vehicle. Figures 4, references 2 Russian.
[124-6508]

NUCLEAR ENERGY

SELECTION OF PACKING DESIGN FOR MAIN JOINT OF VVER-1000 REACTOR

MASLENOK, B. A. and ZADEREY, N. N., candidates of technical sciences

[Abstract] The complex task of sealing the main joint of a nuclear reactor involves finding a reliable solution for the various reactor modes including breakdowns and shutdowns. Two packing design variants (tubular and rod packing) were considered for the VVER-1000 reactor and were tested in a model with approximately real dimensions with the flange of the vessel to be sealed at the joint with the reactor cover. There were arrangements for the introduction of the rod and tubular packing to be compared and pressure gaging of pack leakage. In the first cold testing stage, the vessel was closed, filled with water and brought to 25.6 MPa and then pressures were varied from 0-16.4 MPa at a temperature of around 20°C. The second or hot stage involved 10 cycles with temperatures of 60-322°C and pressure variations of 3.58-16.4 MPa. The coolant heating speed was around 20°/hour. Testing showed the rod packing to be significantly better. It is also easier to manufacture and repair, is cheaper, and has been used for a long time at the Novovoronezhskiy Nuclear Power Plant. Figures 3.
[127-12497]

DYNAMIC SUPPORTS FOR ANTISEISMIC PROTECTION OF NUCLEAR POWERPLANT EQUIPMENT AND PIPES

GLEBOV, V. P., KAZNOVSKIY, S. P., doctors of technical sciences, and SELEZNEV, V. P. and SMIRNOV, N. V., engineers

[Abstract] A study is made of mechanical and hydraulic antiseismic shock absorbers developed by certain industrial firms in the United States, Japan and West Germany and widely used at nuclear powerplants. The most widespread

4

type of shock absorbers designed for loads of 50 to 5000 kN and higher are hydraulic shock absorbers. The creation of mechanical antiseismic shock absorbers is said to be a new and promising trend. Their use is particularly effective for mounting of pipes in inaccessible locations where loads anticipated are 10 to 500 kN. Figures 5.
[128-6508]

SEISMIC TESTING OF A NUCLEAR POWERPLANT LEAK COOLER MODEL

YES'MAN, V. I., YEFREMOV, A. I., candidates of technical sciences, and KERIMBAYEV, S. D., engineer

[Abstract] The cooler model tested was a precise copy of an actual nuclear powerplant leak cooler made of steel in 1:5 scale. A photograph of the device is presented. Modeling of seismic loads was performed using a rigid three-component vibrating platform type ST III-200, operating at up to 200 Hz in each of the three directions with continuous, independent regulation of frequency and amplitude, thus varying the acceleration and time of application of each process. The model studies were used to obtain values of acceleration at individual points in the model with separate and combined application of longitudinal, transverse and vertical oscillations. The most stressed zones of the structure were determined to be the supporting elements. The maximum stresses did not exceed the tolerable stresses for the structural materials used. There were practically no stresses on the surface of the cooler. Figures 3, references 3 Russian.
[128-6508]

STUDY OF SEISMIC STABILITY OF EQUIPMENT OF FIRST LOOP OF NUCLEAR POWERPLANT WITH WATER-WATER REACTORS

VETOSHKIN, V. A. and SHCHUKIN, A. Yu., engineers

[Abstract] Basic statements are presented from the method of mathematical study of the seismic stability of equipment in the primary loop of a nuclear powerplant with water-cooled, water-moderated reactors on the example of a saturated steam generator. Studies were performed for the maximum credible earthquake, intensity 9 on the Soviet standard scale. Calculation for vertical seismic stress allows determination of the insufficient strength of the steam generator supporting structure. The use of the method can allow analysis of calculation models rather precisely reflecting the actual

structure, development of well-founded and effective antiseismic measures, assuring seismic stability of equipment, and increasing the overall sophistication of planning of nuclear powerplant power equipment. Figures 3, references 6 Russian.
[128-6508]

PROBLEM OF ASSURING SEISMIC STABILITY OF NUCLEAR POWERPLANT POWER EQUIPMENT AND MEANS OF ITS SOLUTION

KOZNOVSKIY, S. P., doctor of technical sciences, and FILIPPOV, G. A., doctor of technical sciences, professor

[Abstract] Seismic stability means the capacity of equipment and structures to retain certain properties such as tightness of seal, strength, lack of residual shape change disrupting normal operation, repairability, nuclear and radiation safety under the influence of seismic loadings. The solution of the problem of assuring seismic stability of nuclear powerplants requires the solution of three main problems: prediction and quantitative estimation of seismic danger; development of seismically stable equipment; creation of special technical devices for protection of equipment from seismic effects. This requires particularly optimization of the design of equipment and technical solutions based on careful analysis of safety problems, economy and the level of calculated risk. Selection of optimal means of antiseismic support and improvement of shock absorbing structures in order to increase their economy, effectiveness and reliability are component parts of the problem. References 3: 2 Russian, 1 Western
[128-6508]

CALCULATING DOSE ABSORBED BY N_2O_4 COOLANT FROM GAMMA RAYS IN REACTOR CORE

MASLENNIK, I.S., NESTERENKO, V.B. and NICHIPOR, G.V., Institute of Nuclear Power Engineering, BSSR Academy of Sciences

[Abstract] While it is usually assumed in estimating the dose absorbed in a coolant that the dose is governed by the direct interaction between the gamma photons and the gas atoms, this assumption fails to consider the conversion of gamma radiation when it interacts with the walls of fuel rods and N_2O_4 coolant. This interaction results in the generation of Compton and photoelectrons in the steel of the walls of the gas gaps of the reactor

cooling channels and in the coolant itself; the interaction of these electrons and the gas also determines the radiation energy absorbed by the coolant. To calculate this gamma radiation dose rate in a reactor core, the spectral and group gamma fluxes must be found in the core, a consideration given little treatment in the literature, since it is not essential in the design of reactor shielding. The data on gamma flux attenuation in N_2O_4 coolant are obtained by breaking the gamma radiation spectrum down into 8 groups, in which the lower energy boundary in each group is half that of the next higher group. The electron emission spectrum arising with the interaction of photons and the material (Compton and photoelectrons) is approximated by a beta radiator Fermi spectrum. It is shown that the dose rate received by the N_2O_4 in the core is determined by the interaction of electrons with the gas, where the electrons come from the walls of the gas space. The major part is played by low energy electrons; at coolant densities of up to $1.29 \cdot 10^{-2}$ g/cm^3, the dose rate is a linear function of the density, thereafter becoming nonlinear. These interaction effects have a significant impact on the dose received by the N_2O_4. Because of the increase in the concentration of excited molecules, an increase in the chemical reaction rates for dissociation-recombination processes can be anticipated in the laminar sublayer of the cooling gas near the wall. The importance of these factors for the design and operation of nuclear power plants with a dissociating coolant requires that special experiments be performed to check the computational model of this paper. Figures 2, tables 2, references 5 Russian.
[173-8225]

METHOD OF CALCULATING TEMPERATURE PROFILE IN FUEL ROD WITH ECCENTRIC POSITIONING OF FUEL

VOROB'YEV, M.A., KULISH, G.V. and KHAZHMURADOV, M.A., Physics and Engineering Institute, UkSSR Academy of Sciences

[Abstract] Thermal parameter calculations for fuel rods using circular tablets in nuclear power stations generally assume that the core, jacket and temperature fields are symmetrically centered in the rods. Since this is not feasible, this paper mathematically analyzes a fuel rod in which the fuel tablets are off-center in the casing. R-function theory is applied to the determination of the steady-state profile of the temperatures in such fuel assemblies. The detailed mathematical treatment is illustrated with the application of the technique to temperature profile computations for the fuel rods of a BGR-300 fast helium-cooled reactor. It was assumed that the fuel briquette was displaced from the center by 0.009 cm, providing a minimum gap of 0.001 cm between the edge of the fuel tablet and the jacket. The algorithm is written in PL-1 and the program running time on a YeS-1022

computer does not exceed 13 min. The histogram of the temperature
distribution is plotted and it is noted that the off-center positioning of
the fuel in the jacket causes a redistribution of the heat flux and con-
siderable azimuthal nonuniformity of the temperature field is observed.
The concomitant hot spots in the fuel rods, temperature stresses,
assymetrical restructuring of the fuel configuration and nonuniform conden-
sation of volatile fission products on the jacket can all have a negative
impact on rod viability. Figures 2, references 9 Russian.
[173-8225]

DESIGN AND DEBUGGING OF DRIVES OF SELF-CONTAINED REACTOR CONTROL SYSTEM
ACTUATING MECHANISMS

GAYGEROV, O.P., ZIMIN, Yu.A., ZHEMCHUZHNIKOV, G.N. and NEDBETSKIY, B.M.

[Abstract] The stringent requirements placed on the actuating mechanisms
of self-contained drives in reactor control systems of nuclear electric power
stations are best met by linear electrical stepper motors. Two types of
drives with such motors are used in nuclear equipment: AZ-KS for emergency
protection and compensation and AR for automated control systems. The AR
drives operate at 80 V and the AZ-KS at 140 V with a pulse width of 0.04 s
and repetition rates of 2 and 4 Hz; the holding voltage is 18 V. The AR
and AZ-KS drive motors can handle loads of 30 and 50 kgf respectively at
winding temperatures of 150°C. The holding force is no less than 50 kgf.
This paper details the design and performance of these two stepper motor
drives, illustrating the specifications with graphs of the static
characteristics showing the load in kgf as a function of the travel in mm
for single-phase and two-phase circuit configurations at currents between 2
and 15 A, as well as with graphs of the output force in kgf as a function
of both the motor current and pulse voltage for two different waveforms.
Service life and wear studies demonstrate that such drives are suitable in
reactor control systems for nuclear electric power stations. Figures 2,
references 4 Russian.
[173-8225]

INDUSTRIAL TECHNOLOGY

UDC 621.86.067.2

AUXILIARY UNITS FOR ROBOTS

Moscow MASHINOSTROYITEL' in Russian No 1, Jan 84 p 19

[Article in "Mechanization and Automation of Production" section, by
S.I. Kruglov and Yu.V. Mironovski,]

[Text] Feeders of the lifting type (two standard sizes) and a feeder of the
revolving type are designed for flat stock. The units are of the floor type
and are controlled in the automatic mode by the control systems of robotic
systems (RTK's). The stock is secured by readjustable bases or individual
holders.

Technical Data on Lifting-Type Feeders

Specifications	Standard size of feeder	
	No 1	No 2
Maximum dimensions of stock, mm	500 x 450	250 x 200
Minimum diameter of stock which can be fed, mm	150	50
Maximum height of stack of stock, mm	350	350
Stock lifting rate (continuously variable control), m/s	0-0.0046	0-0.0046
Number of holders which can be put in	2	2
Rate of return of lifting unit to extreme lower position, m/s	0.043	0.043
Kind of drive	Electric	Electric
Power requirement, kW	0.5	0.5
Kind of current	a.c.	a.c.
Frequency of current, Hz	50	50
Voltage, V	380	380
Overall dimensions, mm:		
Length	1660	960
Width	600	300
Height	1000	1000
Weight, kg	250	180

Feeders of the lifting type are 2-position: One position is the working position and the other serves the purpose of loading the stock; positions are changed manually.
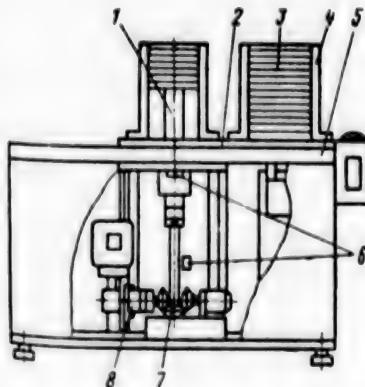
Figure 1.

In setting up the feeder, the stock is removed by the hand of an industrial robot (PR), from the area of the die block placed on the press's die holder, and is fed to the feeder's lifter, 1, which has been moved to the extreme upper position. The required number of supports, 4, are set up for the purpose of securing the stock so that the stock can pass between them smoothly, without jamming. The required number of blanks, 3, are loaded into holders and a support is set up with a microswitch, which monitors the upper level of the stock.

After removal of the top blank by the robot's hand, the stack of blanks is lifted by an amount equal to the thickness of the blank removed. In case the stack of parts is lifted higher than the upper limit, the microswitch issues an instruction to disengage the electromagnetic clutch, 8, linking the lifting drive with the lifter's screw mechanism, 7; lifting of the stock is interrupted until the industrial robot in removing a blank restores the upper limit of the stack.

When the blanks from a single stack have been used, an end switch, 6, monitoring the upper position of the lifter, is operated. The industrial robot ceases to operate and the feeder's lifter is automatically lowered to the extreme lower position. A carriage, 2, is moved manually along guides, 5, so that the second stack of blanks occupies the position of the first, after which the position of the carriage is fixed. Then the cycle is repeated, and the operator has an opportunity to load an empty holder with blanks.

The revolving-type feeder has eight positions, one of which is the working position and the other seven serve the purpose of loading and storing blanks. Positions are changed automatically. The stack of blanks is secured by individual holders.

10

The lifting and lowering mechanisms have been borrowed from the design of feeders of the lifting type and are unified elements. Their operation is also similar to the operation of the like elements of feeders of the lifting type, but the changing of positions in the automatic mode is performed by means of a drive consisting of an a.c. motor, a reduction gear and a crank mechanism. After the lifter is lowered to the extreme lower position, a turning mechanism moves the drum to the left position.

Technical Data on Revolving-Type Feeder

Maximum dimensions of stock which can be fed, mm	180 x 140
Minimum dimensions of stock which can be fed, mm	70 x 30
Maximum height of stack of blanks, mm	600
Lifting rate for stack of blanks (continuously variable control), m/s	0-0.0046
Speed of return of lifting mechanism to extreme lower position, m/s	0.043
Number of holders	8
Kind of drive	Electric
Power requirement, kW	0.6
Kind of current	a.c.
Frequency of current, Hz	50
Voltage, V	380
Overall dimensions, mm:	
Diameter	886
Height	1060
Weight, kg	260

The auxiliary units which have been developed can be used with greatest efficiency in diversified production. They make it possible to form robotic systems for cold sheet-metal stamping based on 250- to 2500-kN model KA and KD presses. The time for readjusting the robotic system when changing from stamping one part to stamping another is from 30 to 60 minutes, including work on replacing attachments.

The use of unified loading devices demonstrated high efficiency of their use in production.

COPYRIGHT: Izdatel'stvo "Mashinostroyeniye", "Mashinostroitel'", 1984

8831
CSO: 1861/219

ROBOTIZED SYSTEM FOR TREATING GEAR WHEELS

[Article in "Mechanization and Automation of Production" section, by
V.M. Gilod, F.I. Kaplunskiy and A.G. Umerenko]

[Text]   Industrial robots are used in heat treating mainly in the operations
of loading and unloading furnaces and salt baths, and also for testing the
hardness of parts and for marking and stocking them.   The robotized system
which has been developed for heat treating gear wheels contains a revolving
feeder, 4, a robot, 3 ("Tsiklon 5.01"), a model I32/80 electrothermic unit, 1,
and a receiving container, 2 (for more details on the feeder see the article
by S.I. Kruglov and Yu.V. Mironovskiy, "Auxiliary Units for Robots," in this
issue of this journal).
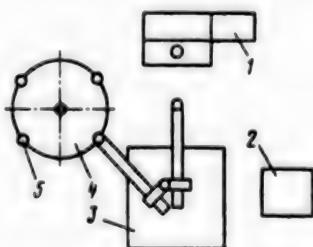
Figure 1.

A holder, 5, with blanks is put into the feeder, from which the robot grasps
a blank and puts it into the electrothermic unit.   Upon the completion of heat
treating, the robot puts the blank into the container.   After complete loading
of the holder, the feeder's table turns and puts the next holder into the
feeding position.

The load lifting capacity of one arm of the robot is 5 kg; the number of
degrees of mobility (without grasping) is from four to six; the robot's
drive is pneumatic.   The maximum height of the stack of blanks in the revolv-
ing feeder is 600 mm and the lifting rate for blanks is from 0 to 0.046 m/s,
and the feeder has an electric drive.

The robotized systems are attended to by an operator who operates the systems and loads holders. With this the equivalent of two people are freed.

MODERNIZATION OF RUNNING GEAR OF CRANE

[Article in "Repair and Modernization" section, by A.I. Zhabin and V.A. Romashchenko, candidates of technical sciences, and B.M. Kivenson, engineer]

[Text] A major shortcoming of the running gear of overhead traveling and traveling gantry cranes is the increased wear of running wheels, in particular, of the flanges, as well as the wear, associated with this, of the lateral faces of the rail head.

As an analysis has demonstrated, the service life of wheels and rails is extended by using additional devices which eliminate sliding friction of the flanges against the rails, by imparting to the running gear the ability to self-balance the crane in the process of its moving along the rail track, and by making possible self-alignment of the running wheels in the horizontal and vertical planes.

Sliding friction of the flanges against the lateral face of the rail can be totally eliminated by installing lateral rollers, 1 and 3 (fig 1), on each wheel, on conical rolling-contact bearings on both sides of the rail, 2. When the crane shifts and becomes misaligned, the lateral rollers alternately interact with the lateral faces of the rails, i.e., sliding friction is replaced by rolling friction. With this, wear of the lateral faces of the rails and running wheels is reduced. As a result, the service life of the wheels and rails increases. However, the use of lateral rollers is restricted for the following reasons:

When they are installed, the overall dimensions of the crane are increased; in particular, the permissible distance (not less than 60 mm) from projecting parts of the ends of the crane to building pillars and walls is not maintained. Therefore, sometimes a roller, 3, with a reduced diameter is installed on the outside of the rail, 2.

Lateral rollers are complicated to make and install.

Considerable axial forces originate when the rollers act on the rail. Nominally, the lateral load on the rail when the crane shifts and becomes misaligned relative to the track beneath the crane equals 100 to 200 kg per ton

of the load on the crane's running wheel, but in practice it reaches 0.3 to 0.5 times the vertical load on the rail.

As a result of the development and accumulation of fatigue cracks, to which forced reduction of the diameters of rollers is conducive, the danger arises of their failure and falling from a great height.
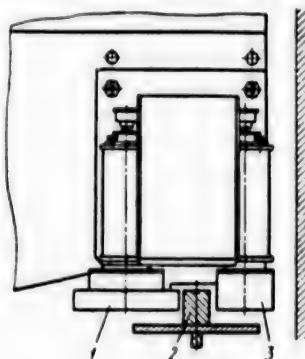
Figure 1.

The use of lateral rollers on overhead-track hoists with a load lifting capacity of two tons with a separate drive is of interest. In spite of the presence of lateral rollers, 2 (fig 2), installed in cantilever on each wheel, 1, in misalignment of overhead-track hoists, the vertical walls of the channels, 3, touched the flanges of the H-beam, 6, which involved losses for overcoming sliding friction and intense wear of the channels, 3, and H-beam, 6. In addition, motors and the reduction gears of the drive of the mechanism for moving overhead-track hoists often failed. In order to eliminate the force of sliding friction in end beams, eight lateral rollers, 4, were installed, which consist of an axle with two ball bearings and a tire, 5, with a working surface of hardness HB 350 to 400.

Loads on the drive and running wheels were reduced by a factor of 10 to 12 with installation of the lateral rollers. The experience of using such overhead-track hoists has confirmed the effectiveness of this modernization solution.

A successful solution to the problem of the longevity of working wheels and rails has been to provide for the self-balancing of the running gear of a crane in the process of its motion, which is achieved by the use of bevel-type crane wheels. The reason for their limited use at the present time is apparently failure to surface harden by means of induction hardening the races of running wheels. A hardened layer with hardness of HB 400 to 500, 2 to 4 mm thick, as a rule, pits, and earlier in bevel wheels (in connection with the more intense transverse movements of the crane) than in cylindrical wheels. Another reason for the limited use of bevel wheels is the mass changeover of plants to the production of cranes with an individual travel mechanism drive, since it is not possible to achieve a balancing effect with

15

the absence of a brace between the driving bevel wheels. Bevel wheels which have been installed with a raceway surface hardness of HB 220 to 250 rapidly flatten and take on a cylindrical shape.
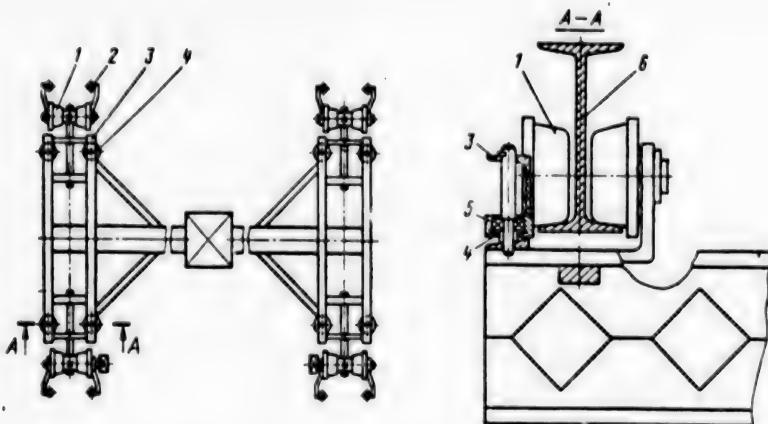
Figure 2.

A new method of installing bevel-type running wheels has been developed and improved for cranes with a central drive; this method has been named the "reverse bevel" method, i.e., the drive wheels have the apexes of the bevels directed away from the shop's bay axis, and the free wheels, the opposite (cf. MASHINOSTROITEL', No 7, 1979, p 4). The use of the "reverse bevel" makes it possible to align the crane and to reduce by a factor of three to five the amplitude of variations in the mechanical trajectory. Furthermore, the friction of flanges against the rails is practically eliminated and the service life of flanges is increased by a factor of three to four, and in some cases by more than a factor of 10.

It is necessary to observe the following conditions when using a "reverse bevel":

The running wheels must be secured against axial motion.

The total clearance between the flanges and the rail head must be not less than 30 to 40 mm.

The mutual misalignment of bevel running wheels must be not greater than 0.003 radian, and the requirements for the precision of their installation are lowered by one order of magnitude.

The crane tracks must be made of crane or railway rails and the use of beams is not permitted.

With the installation of bevel running wheels, the service life of cranes was increased by a factor of three to five.

An experiment in the use of bevel running wheels on an overhead traveling crane with a load lifting capacity of 75/20 tons is of interest. The crane's

span was 22.5 m, its rate of travel was 80 m/min, and its operating mode was the average. The principal shortcoming of the crane was the short service life of the cylindrical running wheels. For the purpose of eliminating intense wear of the flanges caused by misalignment and shifting of the crane when it moved, bevel wheels, 1, with the apex of the bevel directed away from the axis of the span were installed on the driving equalizers, 2 (fig 3), and cylindrical running wheels, 3, on the free equalizers. The taper of the bevel wheels was 1 : 8. Worn running wheels made of grade 45 steel restored by building up according to the standard process were used as stock. The rate of wear of flanges was thereby reduced by a factor of 12 to 15.
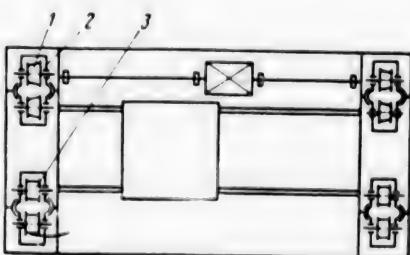
Figure 3.

It must also be mentioned that the use of a "reverse bevel" on flangeless running wheels makes it possible to practically eliminate axial loads on lateral rollers. The self-alignment of running wheels in the horizontal and vertical planes, which is achieved by placing them on spherical-race thrust bearings, as well as by increasing the axial travel of driving and driven running wheels to 5 to 10 mm, lengthens the service life of running wheels and rails.

The longevity of running wheels and rails is made possible also by using separated 3-support gantries in overhead traveling cranes instead of 4-support rigid-design gantries. For example, a change to a statically determinate system is achieved by using two L-shaped 3-support semi-gantries which are hinged. With this, a specific level for loading each of the running wheels is made possible and the relative freedom of movement of the semi-gantries in the horizontal and vertical planes makes contact between all running wheels of the crane and crane rails constant and reliable and makes it possible to operate even on curved sections of the crane tracks. As a result, the power consumption of the motors for the moving mechanism was reduced, and the power was distributed equally over the motors. The service life of running wheels made of grade 55G2 steel was lengthened by a factor of eight.

The directions indicated in this article for modernizing the running gear of cranes do not require considerable additional investment and can be introduced at each enterprise in the regularly scheduled replacement of running wheels.

8831
CSO: 1861/219

CONTROLLING PNEUMATIC DRIVE PISTON MOTION FOR AUTOMATIC MANIPULATOR

[Article by candidate of technical sciences A.A. Paroy and engineer
A.M. Lizunov]

[Text] The actuating elements of the pneumatic drive of an automatic manipu-
lator are primarily controlled in accordance with a stringent cyclical
program using stops as the end position locators. For this reason, it is
necessary to design control systems for the drive piston motion such that
simultaneously with the arrival of the piston at the end position, a
specified type of motion would be produced depending on the drive parameters.

A pneumatic drive piston moves when a pressure gradient is present in the
drive chambers. The manipulator is brought to the end position when the
drive piston brakes, which is accomplished by creating a braking force in the
discharge chamber of the drive.

We shall analyze the dynamics of a pneumatic drive, in particular, a function
governing the change in the velocity of the piston, $\dot{x}$ and its acceleration $\ddot{x}$
(Figure 1).

The piston travel is broken down into three periods: the run-up of the piston
at a definite (most often steady) rate (the time segment t_I), the motion of
the piston at this speed until the onset of braking (t_{II}), and the braking
of the piston (t_{III}).

We find the following from the equations of motion of the piston prior to the
start of braking and during braking, taking into account the fact that
$F \simeq F_B$:

$$\ddot{x} = \frac{(p - p_B)F}{m} - \frac{P}{m};\tag{1}$$

$$\ddot{x}_T = \frac{(p_{BT} - p_T)F}{m} + \frac{P}{m},\tag{2}$$

where p and p_B are the compressed air pressures in the working and discharge chambers respectively prior to braking; p_T and p_{BT} are the compressed air pressures in those same chambers during the braking period; F and F_B are the piston areas on the rod and rodless chamber sides respectively; P is the load on the piston; m is the mass of the translationally moving parts; $\ddot{x}$ and $\ddot{x}_T$ are the piston accelerations prior to and during braking.
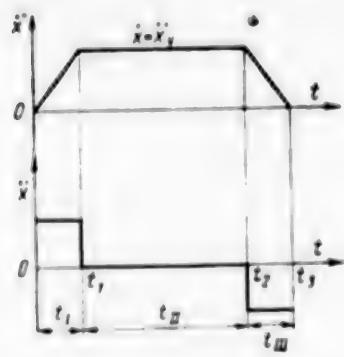
Figure 1. Curves for the change in the dynamic drive parameters.

It can be seen from (1) and (2) that the piston moves and decelerates by means of a pressure gradient on both sides of it:

$$\Delta p = (p - p_B); \quad \Delta p_T = (p_{BT} - p_T).$$

The rate of piston travel is:

$$\dot{x} = \int_0^t \ddot{x}(t)\,dt. \tag{3}$$

Then, correspondingly for the sections:

$$\dot{x}_1 = \int_0^{t_1} \ddot{x}_1\,dt; \quad \dot{x}_8 = \int_{t_1}^{t_8} \ddot{x}_8\,dt; \quad \dot{x}_T = \int_{t_8}^{t_8} \ddot{x}_T\,dt. \tag{4}$$

Taking (1) and (2) into account,

$$\dot{x}_1 = \int_0^{t_1} \left[\frac{(p - p_{B_1}) F}{m} - \frac{P}{m} \right] dt; \tag{5}$$

$$\dot{x}_8 = \int_{t_1}^{t_8} \left[\frac{(p - p_B) F}{m} - \frac{P}{m} \right] dt; \tag{6}$$

$$\dot{x}_T = \int_{t_8}^{t_8} \left[\frac{(p_{BT} - p_T) F}{m} + \frac{P}{m} \right] dt. \tag{7}$$

Consequently, for automatic control by a working drive element, a system is needed which tracks and regulates the change in the speed in accordance with an optimal graph for each section with precise stopping of the translationally moving parts of the drive in the end position. The automatic control system should be simple to service, reliable in operation, control the drive efficiently and have good performance for the given pressure gradient; at the end of the travel, it should also assure the requisite stopping precision without shocks or rebound.

Such drive parameters as the compressed air pressure in the main line, p_M, the mass of the translationally moving parts, m, the load on the piston P

19

and the diameters of the rod and the piston are constants, while the parameters p, p_B, p_T and p_{BT} are regulated by changing the cross-sectional areas of the inlet f and discharge f_B openings.

Depending on the way in which the braking force is produced, the following methods of control and regulation can be proposed:

1. The piston is accelerated in the first section up to a speed equal to its steady-state value ($\dot{x} = \dot{x}_y$) and moves in the second section at this velocity until the start of braking. When the coordinate for the start of braking is reached, x_H, the piston velocity ($\dot{x}_H = \dot{x}_y$) drops off to zero.

The problem of optimal control consists in determining the points in time when the piston reaches the velocity $\dot{x} = \dot{x}_y$, tracking this velocity until the start of braking, determining the coordinate for the start of braking and tracking the piston velocity decline $\dot{x}_T$ down to zero.

In this case, the ratio of f and f_B is controlled in the first section; in the second, this ratio becomes different and is kept constant until the onset of braking, x_H. At the onset of braking, the cross-sectional area of the discharge opening is either completely or partially covered over ($f_B = f_{BT}$). The control problem consists in maintaining the new ratio of f_{BT} to f.

In this case, instructions must be generated to cover over or open up the cross-sectional areas of the input and discharge lines both at the start of travel and when the piston reaches the speed $\dot{x}_y$, when braking, and in the end, when the speed reaches zero.

2. The piston is accelerated in the first section up to a speed equal to the steady-state value $\dot{x} = \dot{x}_y$ and travels at this speed in the second section. When the piston reaches the coordinate for braking x_H, the piston speed begins to drop from the value of $\dot{x}_H = \dot{x}_y$ down to $\dot{x}'$, i.e., the values of the velocity at which the acceleration takes on a value of $\ddot{x} = \ddot{x}'$.

The problem of optimal control consists in determining the points in time when the piston reaches the velocity $\dot{x}_y$, tracking this until the onset of braking, in determining the coordinates for the onset of braking and tracking the decrease in the piston speed from $\dot{x}_H = \dot{x}_y$ down to $\dot{x}'$, in determining the coordinates at which the acceleration takes on the requisite value, and the piston takes on a value of $\dot{x}'$, as well as in tracking the uniform drop in the piston speed from the value of $\dot{x}'$ down to zero.

In this case, instructions must be generated to cover (or open) the cross-sectional areas of the input or discharge lines both at the start of piston travel and when the piston reaches the velocity $\dot{x}_y$, as well as to completely cut off the cross-section of the discharge channel at the moment the piston reaches the coordinate for braking onset x_H and keep it cut off; an instruction must also be generated for the sudden opening of the cross-section of the discharge channel at the point in time when the piston reaches the coordinate x' and to stop the piston when it reaches a velocity of $\dot{x} = 0$.
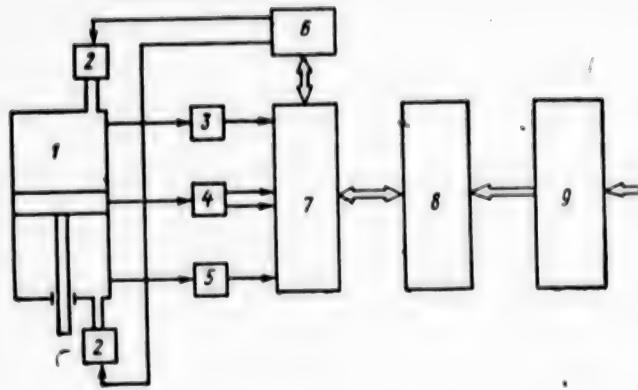
Figure 2. Block diagram of the control system.

In this case, the ratio between f and f_B is controlled in the first section; in the second section, this ratio becomes such that the steady-state travel of the piston is assured. At the start of braking, the cross-sectional area of the discharge channel is completely covered and $f_{BT}/f = 0$. This ratio is maintained in the section $x_H - x'$, and then a new ratio of the areas is established, f_{BT}^0/f (where f_{BT}^0 is the value of the discharge channel cross-section at the point in time when the channel is suddenly opened). The ratio of the areas is varied thereafter so that the law governing the change in the cross-sectional area of the discharge channel is observed from $f_B = f_{BT}^0$ down to $f_{BT} = 0$.

3. The piston is accelerated in the first section up to a speed $\dot{x} = \dot{x}_y$ and moves at this speed until the onset of braking. When the piston reaches the coordinate x_H, an additional quantity is compressed air is fed into the discharge chamber, because of which, the piston velocity begins to drop from the value of $\dot{x}_H = x_y$ down to zero.

The control problem consists in determining the points in time when the piston reaches the velocity $\dot{x}_y$, tracking this velocity until the start of the input of the additional quantity of compressed air (when the piston reaches the coordinate x_H) and then tracking the drop in the piston velocity from the value $\dot{x}_H$ down to zero. In this case, instructions must be fed in to close off the cross-sectional area of the discharge channel ($f_B = 0$), connect the discharge chamber to the main line ($f_{BT} = f_{kl}$), and stop the piston when it reaches the speed $\dot{x}_k = 0$.

4. The piston is run up to a speed of $\dot{x} = \dot{x}_y$ in the first section and travels at this speed until the onset of braking. When the piston reaches the coordinate for the start of braking, $x = x_H$, the chambers are repeatedly switched in alternation.

The control problem consists in determining the points in time for the switching of the chambers (including the first switching when $x = x_H$), and then tracking the drop in piston velocity in each switching section, and on the whole from the value $\dot{x}_H$ down to zero.

21

When determining the coordinate for the onset of braking, x_H, an instruction should be fed in for the first change in the cross-sectional areas of the input and discharge lines ($f \rightarrow f_B$, $f_B \rightarrow f$), and then for their repeated alternate switching, as well as when the piston velocity reaches zero or a preset value (some steady-state braking rate, $\dot{x}_{yT}$).

5. When the braking of the pneumatic drive piston is accomplished by connecting an additional capacity to one of the chambers and cutting off the discharge cross-section from the other chamber, equal acceleration travel of the piston takes place up to a value of the velocity of $\dot{x} = \dot{x}_H$. When the piston reaches the coordinate x_H, the piston begins to decelerate and the velocity drops from $\dot{x}_H$ down to zero.

The control problem consists in tracking the piston travel until it reaches the velocity $\dot{x}_H$ (determining the coordinate x_H) as well as the drop in the piston speed from the value $\dot{x}_H$ down to zero.

In this case, an instruction must be generated to cut off the cross-sectional area of the discharge channel (at the point in time when the piston reaches the coordinate x_H).

It can be seen from all of the cases described here that the major task in the realization of a particular optimal control technique consists in determining the point in time (or coordinate of the point) for the onset and conclusion of deceleration. With the second approach, besides determining the coordinate x_H, one must also determine the coordinate x'.

As far as the fourth control method is concerned, here one must determine the period (coordinate) of switching the areas in addition to determining x_H.

When tracking the coordinate x_H, the signal must instantaneously be generated to either close off the discharge channel area from a value of f_B down to f_{BT} (for the first two methods) or to cut off the cross-sectional area of the discharge opening and make the connection by means of the cross-section of the main line (for the third control method), or generate a signal for the alternate connection of the air distributor and the replacement of the cross-sectional area of the feed line with the cross-section of the discharge line (the fourth method).

The instruction when the piston reaches the coordinates x_H, x' or $\dot{x}_K$ can be supplied either from piston position sensors or based on the time of piston travel or the piston speed.

The mathematical function takes the form of an ensemble of solutions to equations which describe the piston motion along the optimal graph as a function of the values of p, p_B and $\ddot{x}$, taken as applied to the quantities x and t. In the conversions, the most interesting functions are the unique functions [$\dot{x}(x)$, $p(x)$, $p_B(x)$, $p_T(x)$, $p_{BT}(x)$, etc.]. A numerical value of $\dot{x}_i$ uniquely corresponds to each specific value of $\dot{x}_i$ in the function $\dot{x}(x)$.

Tracking these parameters and the instructions related to them for the corresponding actuating elements provides for an automatic control system (Figure 2), the major components of which are: the pneumatic drive 1, the controlled regulating chokes 2, the sensors for the compressed air pressure in the working chamber 3 and the discharge chamber 5, the travel and speed sensor 4, the control unit 6, the block for processing the equations of motion 7, the arithmetic logic unit 8 and the unit for entering the initial data and recording it in the memory 9.

Block 9 is broken down into a program memory and a data memory. The coordinates of the onset of braking and the end of motion are determined in block 8. The steady-state values of the piston speed prior to braking and during braking are also calculated here.

The actual and computed values of the parameters are compared in unit 7 and the error signals are converted to digital form.

In unit 6, the instructions are generated and fed out for the execution of the motion periods: the start of motion, the start of braking, stopping, as well as for the closing or opening of the regulating valves.

Sensor 1, which is a contact transducer for converting the linear travel to rotational motion and makes it possible to measure the angles of rotation corresponding to this rotation, is used to measure the current coordinates of the piston position, as well as its rates of travel. This is a pulse (or code) rotation angle sensor.

The individual assemblies and units for the control system have been designed at the present time and their test results have been obtained. The system will be completely installed in the automatic manipulators of a robot equipped production complex intended for the cold stamping of parts.

8225
CSO: 1861/198

DETERMINATION OF MOMENTS OF INERTIA OF COMPLEX SHAPED PARTS

KOVALEV, S. L., graduate student

[Abstract] A method is suggested for determining the moments of inertia based on the use of modern computer equipment and most effective for parts of complex shape. An equation is presented that can be integrated with respect to the volume of the part. The method provides good computational accuracy regardless of the specific computer or programming language used and practically eliminates manual computations. Figure 1, references 4 Russian.
[132-6508]

STUDY OF AXIAL BEARINGS WITHOUT OIL BATH WITH RADIAL COOLING OF BLOCKS

ZARETSKIY, Ye. I., SEREZHKINA, L.P., candidates of technical sciences, PIPIN, A.A., and TSYBUL'NIK, I.I., engineers

[Abstract] Losses by friction in axial bearings of fossil-fuel and nuclear electric plant turbines amount to 0.1-0.17% of the developed power. A large part of the power losses occur because of disk friction. In order to eliminate friction and increase the efficiency coefficient of the turbine the Kharkov Turbine Plant developed axial bearings without oil baths with individual lubricant supply for each block. In a bearing with a diameter of 585 mm and 1200 cm^2 working surface, a two-layer box made of thin plate with a rigid base is established and linings form input and output chambers and slot grooves. Oil is forced into the cooling channel and over the working surface and passes from one block to the next. Effectiveness of the oil feed was tested by removing outlet channels and this led to a load-carrying capacity loss of 30%. Transport is effected by a pressure differential. Experimental results show superiority of the method over an oil bath with significant temperature advantages. Load-carrying capacity, with improved block bases, attained 900 kN. The complex channels may clog and carrying capacity could be reduced by one-half if oil is not kept clean. Figures 4.
[127-12497]

CUTTING STRUCTURAL MATERIALS IN VACUUM

PETRUKHA, P. G., BESPAKHOTNYY, P. D., KOZINER, Yu. D. and ORLOV, V. I.

[Abstract] A series of experiments was performed to study the influence of
cutting rate and thickness of the layer being cut on cutting force and
deformation of the layer separated during cutting in a deep vacuum without
cooling. Flat specimens were made of materials with various properties,
including titanium, copper, aluminum and steel. Cutting tools included
high speed steels and hard alloy plates. The process was one of free
orthogonal cutting at 13 to 508 mm per minute, thickness of separated layers
0.3 mm, width 2 mm. Low speed cutting reduces the influence of temperature
in the cutting zone on the deformation process. Another series of experi-
ments was used to study the influence of various degrees of vacuum on cutting
force, the process of deformation of the metal in the cutting zone, processes
of friction and tool wear. It was found that as vacuum increased, the most
active wear occurred near the cutting edge. All the parameters studied
increased with increasing vacuum, a result of activation of adhesion and dif-
fusion processes in the contact zone. Figures 3, references 3 Russian.
[124-6508]

METHOD OF MACHINING CONCAVE PART SURFACES ON FIVE-COORDINATE NUMERICALLY
CONTROLLED MILLING MACHINES USING COMPUTER AIDED TECHNOLOGICAL PROCESS DESIGN

VASILENKO, B. N.

[Abstract] A study is made of machining of concave surfaces of parts by
milling with tools whose cutting edges are on their end surfaces. Programmed
control of the angle of the tool with respect to the part is equivalent to
control by changing the curvature of the end surface of the milling cutter.
Consequently, for each point on the surface of the part it is possible to
select values of tool angle for which the curvature of the end portion of
the tool is equal to the curvature of the concave product surface. Ob-
viously, the geometric parameters of the tool selected determine the
possible range of change of curvature of this surface. This question is
analyzed in detail. Utilization of the factors considered in this article
can significantly increase the productivity of this process of milling
concave surfaces. Figures 2, references 5 Russian.
[124-6508]

DYNAMICS OF MANIPULATOR CONSIDERING COMPLIANCE OF HINGES

GORINEVSKIY, D. M., Moscow

[Abstract] A study is made of a manipulator consisting of N elements con-
nected in series by ball joint hinges. The masses and moments of inertia
of the elements are assumed known. The change in angle in each joint is
achieved by independent drives. It is assumed that in the clamp at the end
of the manipulator there is a load, the mass and inertial tensor of which
are also known. It is considered that external forces and moments are
absent. One of the degrees of freedom is considered non-ideal, in that the
angle in one of the joints is the sum of the programmed angle and a
deviation from the program. Two examples of specific potential deformation
energy are studied to illustrate the method proposed. References 3 Russian.
[151-6508]

THERMAL CHARACTERISTICS OF PLASMA REACTORS WITH MULTI-JET CYLINDRICAL AND
CONICAL MIXING CHAMBERS

BUROV, I. S., YERMOLAYEVA, Ye. M., ZABRODIN, V. K. and MOSSE, A. L.
Institute of Heat and Mass Exchange imeni A. V. Lykov, Belorussian Academy
of Sciences

[Abstract] The influence of some characteristics of the high temperature
flux on heat losses in the wall are investigated, and efficiency in the
basic types of mixing chambers - cylindrical and conical - is compared.
Cylindrical chambers made it possible to produce high temperature gas fluxes
with a uniform texture profile, while conical mixing chambers have better
efficiency for the same initial power. References 7 Russian.
[167-6900]

ADAPTIVE MICROPROCESSOR SYSTEM FOR CONTROLLING ROBOT ELECTRIC DRIVE

CHINAYEV, P. I., doctor of technical sciences, CHEKALIN, V. G., and UL'MASOV, Kh. U., candidates of technical sciences

[Abstract] An individual channel of an adaptive electromechanical system is examined as an example of the use of microprocessors to control multi-section electromechanical robots. The use of an adaptation loop to achieve good control system performance is described. The microprocessor system is a general purpose one designed for use with various thyristor and transistor rectifiers, inverters, frequency converters and AC and DC motors. The system provides adaptive control of electric drives subjected to varying external loads and moments of inertia associated with variation in the configuration of sections of an electromechanical robot. Figures 4, references 8 Russian.
[202-6900]

MULTICRITERIAL SYNTHESIS OF INFRASTRUCTURE OF EXTERNAL SPACE

PAVLOV, V. V. and VORONIN, A. N.

[Abstract] Multicriterial synthesis of the infrastructure of the geometric space within which a mobile robot operates is examined. The problem of constructing the infrastructure of a system for controlling plane movement of an object on the x-y plane is considered, with allowance for restrictions in the form of forbidden regions and movement of other objects in the same region of the plane. The task of the control system is to move the object in question from one point to another under given conditions. The approach used to compute the path length, the distance to limits and the distance to other moving objects is described. An expression is given for generalized estimation of the trajectory; the infrastructure of the space within which the intelligent robot acts is represented as the direct product of a number of sets. Figures 3, references 7 Russian.
[203-6900]

SYNTHESIS OF SPEED-OPTIMUM CONTROL SYSTEMS THAT CONTAIN NONLINEAR COMPONENTS
OF THE INSENSITIVITY AND DRY FRICTION TYPE

KOLESNIKOV, A. A., SHTEYNIKOV, G. A. and CHINENOV, A. G., Taganrog Radio
Engineering Institute imeni V. D. Kalmykov

[Abstract] Despite the fact that nonlinearities such as free play, dry
friction and zones of insensitivity frequently show up in various servo-
mechanisms and drives, almost no research has been published on closed
systems for controlling objects with nonlinear components of this kind.
The authors of this paper consider the problem of synthesizing a control
law for objects that include components of the insensitivity and dry friction
type in their structure. This law is optimum in the sense that it minimizes
the time for transfer of the control object from an initial arbitrary state
within an admissible range to the coordinate origin of phase space. Figures
3, table 1, references 5 Russian.
[139-6610]

INVESTIGATION OF TRANSPORT OPERATIONS OF ERGATIC ROBOT

METLIN, V. Ye., graduate student, and YUSHCHENKO, A. S., candidate of
technical sciences, docent

[Abstract] An examination is made of ergatic manipulation robots, i.e. those
controlled by a human operator. The authors consider the capabilities of
the operator for performing operations by means of semiautomatic manipulation
systems in which the operator has control of the motion of the gripper by
means of a multiple-degree lever, while the signals for controlling the
manipulator drives are computer-generated. It is experimentally shown
that there is a rather narrow range of variation in generalized parameters
of the manipulator control system where the operator can successfully work
and adapt to changes in the parameters of the hardware part of the system.
This range depends considerably on the method of manipulator control, which
may necessitate adjusting the parameters of the control system when
changing from one method of control to another. Conventional mathematical
models of manipulator control systems can be used to determine such general-
ized parameters as the time constant of the system, gain, and damping
constant. These quantities are correlated by analysis of the roots of a
characteristic equation, or the frequency responses of a model of the

system that has been linearized in the vicinity of the corresponding
point. These results can be used to formulate recommendations on synthesis
of a control system with consideration of the work of the human operator.
Figures 3, references 3 Russian.
[134-6610]

SOME PROBLEMS OF OPTIMUM JOURNAL DESIGN FOR DISK-DRUM ROTORS UNDER
ANTISYMMETRIC LOADING

ZNAMENSKIY, N. P. and KOTEROV, N. I., Moscow

[Abstract] The authors consider the problem of optimizing the shape of the
middle surface of the bearing journals of disk-drum rotors. As the problem
of total optimization of the journal is rather complicated, a simplified
version is considered for partial optimization with respect to individual
parameters. An analysis is made of the possible influence that the shape of
the middle surface and the thickness of the journal have on pliability under
antisymmetric loading. The problem reduces to finding a shell with maximum
stiffness and minimum pliability. It is shown that optimum thickness
profiling is the most effective way to increase journal rigidity. The
analysis is based on the formalism of normal integral equations developed
by Birger for calculating antisymmetric deformation of shells of revolution
[I. A. Birger, "Nekotoryye matematicheskiye metody resheniya inzhenernykh
zadach" (Some Mathematical Methods of Solving Engineering Problems),
Moscow, Oborongiz, 1956, 151 pages]. The BESM-6 computer is used for the
calculations. Figures 5, tables 3, references 5 Russian.
[137-6610]

TURBINE AND ENGINE DESIGN

UDC 621.165.001.5

EFFECT OF DIAPHRAGM LEAKAGE ON TURBINE STAGE CHARACTERISTICS

KIRILLOV, I.I., doctor of technical sciences, LAPSHIN, K.L., SADOVNICHIY, V.N., candidates of technical sciences, GAYEV, V.D. and FOMIN, V.S., engineers

[Abstract] Turbine design optimization and the computation of axial forces requires reliable data on the effects of diaphragm leakage on turbine effectiveness. Leakage through the diaphragm packing cannot be avoided in the intermediate stage and reduces the efficiency coefficient. Gas dynamic computations of infiltration effects are based on experimentally grounded equations and there are differences in specialist opinion as to precise determination of energy losses. Therefore, experiments were done with an EVT-2 turbine with a flow meter in which packing rings and turbine wheel disk vents could be varied. Formulas were established for estimating the effects of accumulated energy losses on the efficiency coefficient and for estimating effects on the turbine stage of working fluid infiltration and suction through the rotor blade region. The design problem consists essentially in minimizing efficiency reduction taking into account axial forces on the rotor and in each specific case an optimal design must be selected for handling diaphragm infiltration flow. Figures 4, references 9: 8 Russian, 1 Western.
[127-12497]

ESTIMATE OF FATIGUE STABILITY OF GAS-TURBINE ENGINE COMPRESSOR VANES IN
PROBABILISTIC ASPECT

PROKOPENKO, A. V. and BAUMSHTEYN, M. V., Institute of Strength Problems,
UkSSR Academy of Sciences, Kiev

[Abstract] The paper describes a method of determining the tolerance limits
of durability of structural components based on correct statistical pro-
cedures. The method is illustrated by calculation from the results of tests
of standard prismatic specimens with a crack, and gas-turbine engine compres-
sor vanes made of 14Kh17N2 steel tested under the same conditions of vibra-
tion loading by bending. The experimentally determined durability of the
vanes was within the tolerance range determined from calculations done with
respect to results of tests of the specimens. Table 1, references 6 Russian.
[143-6610]

INVESTIGATION OF GAS-TURBINE ENGINE BLOWER IMPELLER VIBRATIONS WITH CHANGE
IN ENGINE INTAKE CONDITIONS

YELENEVSKIY, D. S. and MALYGIN, V. V., Kuybyshev

[Abstract] The authors study vibrations of low-pressure compression
impellers in multiple-shaft gas-turbine engines in stand tests with dif-
ferent intake conditions. The working vanes of the investigated blowers
had relatively large linear dimensions compared with the disks, and were
equipped with antivibration shroud tips. The test results show that dif-
ferent designs of the engine intake device have a strong influence on the
structure of nonuniformity of gasdynamic flow at the engine intake, and
also determine the vibration behavior of the blower impellers. Resonant
vibrations of the working vanes occur at maximum symmetry of airflow into
the engine. Distortions of intake conditions introduced by segmental inter-
ceptors increase turbulence in the flow section of the blower, resulting in
stochastic vibration response of the blower vanes. It is pointed out that
the occurrence of stochastic oscillations applies to the vibration modes
of the coupled system comprising the disk, shroud tips and blading, and in-
volves a large number of displacement waves along the periphery of the
impeller. Several such modes are excited simultaneously, resulting in
indeterminate distribution of interblade phase shifts. Consequently a change
in the form of exciting loads radically alters the overall dynamic pattern

of behavior of the blower impeller. The results of studies of the vibration state of the blower in engines of various classes were qualitatively identical, which shows that the patterns observed in this research are general in nature. Figures 6, references 4: 3 Russian, 1 Western. [137-6610]

DETERMINATION OF DIRECTIONAL GYRO PARAMETERS

[Article by V.A. Pavlov, Leningrad Institute of Aviation Instrument Making]

[Text]   A method is discussed for determining the
            principal design parameters of a directional
            gyro as a function of the required accuracy
            of its maintaining a specific direction in
            interial space.

Expansion of the range of the practical utilization of the gyroscopic effect
has created a demand for a great number of gyroscopic instruments series-
produced by industry and of various types with respect to purpose. These are
distinguished from one another by the functions performed, design features,
weight and size parameters, duration of operation, and, what is most impor-
tant, the accuracy of readings, on which ever stricter requirements are im-
posed with each year [1]. The limited time allotted for the development of
new modifications has necessitated methods of calculating the parameters of
gyroscopic instruments in the observance of which the device being designed
will guarantee the accuracy required of it.

The first attempts to calculate the parameters of directional gyros were made
as early as the 30's [2]. However, at this time a clear idea did not exist
of the most efficient relationships between the design parameters of a gyro.
Therefore, the method suggested was used then only for preliminary calcula-
tions. Only after the completion of research on the efficient relationships
between the principal design parameters of a gyro did the practical possi-
bility of determining them analytically appear.

Let us imagine a directional gyro (fig 1) around whose OB axis a moment of
perturbing forces, M , is at work. Let us assume the magnitude of this
moment to be produced by the mass of the gimbals, VK and NK; elastic deforma-
tions and temperature strains of parts of the instrument; and by frictional
forces in the supports of its suspension along axis OB. Let us assume that
the angular drift velocity, $\dot{\psi}_d$, can in this case reach a maximum value, de-
termined according to [3, pp 64, 199, 206 and 236] by the equation:

$$\dot{\psi} = -\frac{1}{J\Omega \cos\vartheta} \left[\frac{J_{Bx} - J_n}{2} (\dot{\psi}_a) \cdot \mathrm{tg}\,\vartheta_0 + (m + m_{_B}) \cdot V_x V_z \left(\frac{1}{C_z} - \frac{1}{C_x} \right) \right.$$

$$\left. + g\left[m (e_0 \alpha_{_B} - b_0 \alpha) - m_{_B} f_0 \alpha_{_B} \right] \Delta t + \lambda (G - G_{_{BK}}) \right],$$

where J, J_{Bx} and J_n are the moments of inertia of the rotor, P , relative to the OA axis, and of the gimbals, VK, relative to the Ox axis, and NK, relative to the OC axis; Ω is the angular rotational velocity of the rotor, P , around the OA axis; θ_0 is the mean value of the error angle between the OA and OD axes; $(\dot{\psi}_a)$ is the amplitude of the angular velocity of nutational vibrations of the gyro; m and m_{VK} , G and G_{VK} are, respectively, the mass and weight of the rotor, P , and VK gimbal; V_x and V_z represent acceleration of the instrument's body, KP, along axes Ox and Oz; C_x and C_z are the rigidity of the gyro along the same axes; g is free-fall acceleration; e_0 , b_0 and f_0 are linear dimensions characterizing the relative position of the centers of mass of the rotor, P , and VK gimbal (fig 2); α and α_k are the coefficients of linear expansion of the materials of the rotor, P , and VK gimbal; Δt is the temperature increment within the body of the instrument, KP; and λ is the coefficient of rolling friction in the supports of the suspension along axis OB. Based on the results of the studies presented in [3, pp 159 and 198], it is possible to replace in the original equation the relationships between the principal design parameters by their mean values, determined in practical work:

$$\frac{G_{_{BK}}}{G} \approx \frac{m_{_{BK}}}{m} \approx 0{,}56; \quad \frac{J_n}{J} \approx 2{,}4; \quad \frac{J_{Bx}}{J} \approx 0{,}13$$
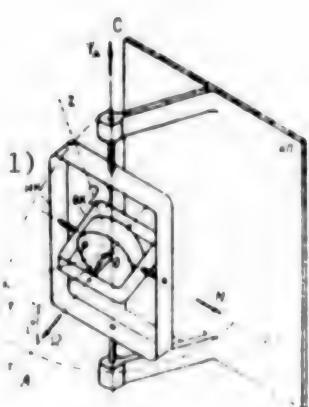

Figure 1.


Figure 2.

Key: 1. NK [outer gimbal]   2. VK [inner gimbal]
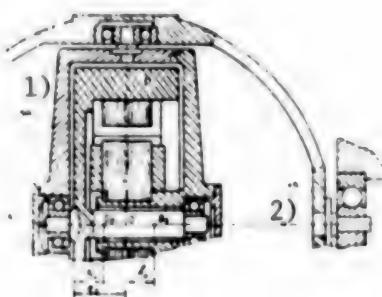
Then, after the obvious transformations,

$$\psi_1 = -\frac{z}{\rho_{\text{н}}^2 \Omega \cos \vartheta_0} \cdot \left[\frac{1.43}{g} \, \rho_{\text{н}} (\dot{\psi}_a)^2 \, \text{tg} \, \vartheta_0 + 2.43m \frac{i_z V_z}{g} \cdot \frac{C_1 \quad C_i}{C_i C_{\text{т}}} + \right.$$
$$\left. + (c_0 \lambda_z - b_0 \lambda - 0.56 f_0 \lambda_z) \Delta t + 1.56 \lambda \right].$$

(1)

where ρ_i is the radius of gyration of the rotor.

The values grouped in square brackets in equation (1) characterize the lengths, ℓ_i , at whose distance from the point of suspension, 0 , (fig 1) external perturbing forces act on the gyro. Taking into account the fact that the range (ψ_a) of variation of the angular velocity of nutational vibrations of the gyro depends chiefly on the moment, M = 156λmg , of frictional forces in the supports of inside axis OB, let us determine the value of the length, λ_1 , due to the first term of the sum to be analyzed. Expressing the moment of inertia, I , in terms of the mass, m , and radius of gyration, ρ_i , of the rotor, it is possible to write:

$$l_1 = \frac{1.43}{g} \, \rho_{\text{н}}^2 (\dot{\psi}_a)^2 \, \text{tg} \, \vartheta_0 = \frac{1.43}{g} \, \rho_{\text{н}}^2 \left(\frac{1.56 \lambda mg}{m \rho_{\text{н}}^2 \Omega \cos \vartheta_0} \right)^2 \text{tg} \, \vartheta_0.$$

whence we find that

$$l_1 = 3.47 g \left(\frac{\lambda}{\rho_{\text{н}} \Omega \cos \vartheta_0} \right)^2 \text{tg} \, \vartheta_0.$$

(2)

The radius of gyration, ρ_i , of the rotor depends on its cross section and for the most widespread case of a hollow cylinder of outside radius R and inside of r = 0.5R [3, p 363] it is determined by the equation:

$$\rho_{\text{н}} = 0.707\sqrt{R^2 + r^2} = 0.79R.$$

(3)

Here, as we know [3, p 119], the increase in radius R is limited by the permissible stress, σ , in the material of the rotor:

$$\sigma = \frac{\gamma \Omega^2}{g} \cdot \frac{R^2 + Rr + r^2}{4} = 0.58 \frac{\gamma \Omega^2}{g} R^2.$$

(4)

where γ is its density.

35

Taking relationships (3) and (4) into account in equation (2), we find

$$l_1 = 3.21\gamma^2 \frac{\lambda}{z} \frac{\lg \vartheta_0}{\cos^2 \vartheta_0}.$$

(5)

The second term in square brackets in expression (1) contains the factor $m\dot{V}_x/C_x$ characterizing [3, p 199] the permissible elastic deformation, Δ_x, of the gyro along axis OA, and the ratio $\dot{V}_z/g$, indicating the ratio, ν_z, of the permissible acceleration to the value of g, in connection with which it is possible to write

$$l_2 = 2.43m \frac{V_x V_z}{g} \cdot \frac{C_1 - C_2}{C_2 C_1} = 2.43\Delta_x \nu_z \frac{C_1 - C_2}{C_2}.$$

(6)

In turn, the coefficient at Δt of the third term of equation (1) can be reduced to the form

$$c_0 a_\kappa - b_0 a - 0.56 f_0 a_\kappa = (c_0 - 0.56 f_0) a_\kappa - b_0 a,$$

in which with precise static balancing of the gyromotor it is necessary to take into account (cf. fig 2) the obvious equation

$$G(c_0 - b_0) = G_{\text{вк}} f_0,$$

according to which

$$b_0 = c_0 - \frac{G_{\text{вк}}}{G} f_0.$$

Substituting the last relationship in the third term of the expression under analysis, (1), we find

$$l_3 = (c_0 a_\kappa - b_0 a - 0.56 f_0 a_\kappa) \Delta t = (c_0 - 0.56 f_0)(a_\kappa - a) \Delta t.$$

(7)

Finally, the fourth term of the considered sum of values contained in square brackets is determined directly from expression (1) by the relationship

$$l_4 = 1.56\lambda.$$

(8)

Taking into account the values found in (5), (6), (7) and (8) of distances λ_i analyzed, it becomes possible to rewrite equation (1):

$$\dot{\varphi}_A = \frac{g}{2\pi^2 \Omega \cos \alpha_x} (l_1 + l_2 + l_3 + l_4).$$

(9)

The equation obtained represents the relationship between the dimensions of the rotor of the directional gyro to be designed and the accuracy required of it, assigned operating conditions and materials selected for fabricating the instrument's parts. Equating the angular velocity, $\dot{\psi}_d$, to the assigned value of $\dot{\psi}_z$, characterizing the accuracy required of the gyro, we take into account the fact that the values of ℓ_i are random. They can vary at random over time both in terms of magnitude and direction. Therefore, under real conditions angular velocity $\dot{\psi}_d$ will always be lower than the value determined by expression (9). Employing the rule of the standard deviation of a sum of random quantities, and relationship (3), and equating $\dot{\psi}_d$ to its permissible value of $\dot{\psi}_z$, from equation (9) we get

$$R = \sqrt{\frac{K}{0.624\,\dot{\psi}_z\,\Omega \cos \theta_0}\sqrt{l_1^2 + l_2^2 + l_3^2 + l_4^2}}\,.$$

This is the expression making it possible to make an analytical determination of the required value of the outside radius, R , of the rotor of a directional gyro as a function of the accuracy imposed on it, under assigned operating conditions, and of the properties of the materials selected.

Bibliography

1. Pavlov, V.A. "Stricter Requirements for Accuracy of Balanced Gyro and Possibilities of Implementing Them," IZVESTIYA VUZOV SSSR: PRIBOROSTROYENIYE, No 1, 1979.

2. Pavlov, V.A. "Method for Preliminary Calculation of Dimensions of Gyro Rotor," TOCHNAYA INDUSTRIYA, No 6, 1940.

3. Pavlov, V.A. "Osnovy proyektirovaniya i rascheta giroskopicheskikh priborov" [Gyroscopic Instrument Design and Calculation Principles], Leningrad, Sudostroyeniye, 1967.

8831
CSO: 8144/0933

DECOMPOSITION IN PROBLEM OF CORRECTING INERTIAL NAVIGATION SYSTEMS

KALENOVA, V. I. and MOROZOV, V. M., Moscow

[Abstract] A study is made of the problem of estimating the state vector
of a linear, steady, observable system. Analysis of equations derived
in the article indicates that all subsystems of the error equations relative
to the vector components are independent, i.e., the equations achieve
decomposition of the initial equation based on components of the measurement
vector. When velocity and position information are used independently, the
correction algorithms which include estimates of only accurately observable
variables have orders 3+5 and 4+4. References 11: 7 Russian, 4 Western.
[151-6508]

QUATERNION ALGORITHMS OF 3-DIMENSIONAL INERTIAL NAVIGATION SYSTEMS

CHELNOKOV, Yu. N., Saratov

[Abstract] A three-dimensional inertial navigation system is studied,
in which three force meters are mounted rigidly to a moving object, generally
in a cardan support. Quaternion equations were derived for an azimuth-
stabilized platform as well as a gyrostabilized platform preserving its
orientation with respect to distant stars. The equations are equivalent
to equations of a perturbed oscillator for arbitrary motion of the object,
to the equations of the harmonic oscillator for Kepler motion of the object.
Of particular interest is the use of two equations in the article for the
solution of an important class of navigational problems in which the distance
from the object to the center of the earth is known as a function of time.
References 7: 6 Russian, 1 Western.
[151-6508]

OBSERVABILITY IN PROBLEM OF CORRECTION OF ARTIFICIAL HORIZON

VAVILOV, S. M., Moscow

[Abstract] Observability of an artificial horizon is used as the basis
for a discussion of the problem of correction of the device, the sensing
element of which is a spherical pendulum with two gyroscopes combined by
means of geared sectors and connected by a spring. The analogy between an
artificial horizon and an inertial navigation system, both of which model
the movement of a Darboux trihedron, is utilized in the analysis. The prob-
lem of correction of the artificial horizon is studied within the framework
of the information approach, the primary stage of which is an analysis of
observability, allowing determination of the possibility in principle of
using the same or other information, estimation of the limiting accuracy of
correction and determination of a class of acceptable algorithms for estim-
ation of the observable parameters. References 6 Russian.
[151-6508]

MOTION OF SATELLITE WITH TOTAL DYNAMIC SYMMETRY AROUND ROTATING ASPHERICAL
EARTH

KOYENOV, D. Z., Tajik State University imeni V. I. Lenin

[Abstract] The problem of motion of a satellite with complete dynamic
symmetry around a rotating aspherical planet was solved in a previous paper
by the author, using the method of Lie transformations [D. Z. Koyenov,
IZVESTIYA AKADEMII NAUK TADZHIKSKOY SSR: OTDELENIYE FIZIKO-MATEMATICHESKIKH
I KHIMIKO-GEOLOGICHESKIKH NAUK, No 1(83), 1982]. Using the expansion of
the generating function of transformations given in the earlier paper, and
considering trigonometric identities for the Andoyer canonical elements,
the author now finds a shorter and more convenient form of expansion that is
used to derive expressions for perturbations of selected canonical elements
that determine the translational motion of a satellite and rotational motion
of the earth with accuracy of 10^{-8}. It is shown that the Delaunay elements
characterizing translational motion of a satellite around the earth undergo
considerable perturbations due to the figure of the earth. References 3
Russian.
[138-6610]

EXISTENCE OF PERIODIC MOVEMENTS NEAR RESONANCES FOR HEAVY GYROSTAT WITH ONE
STATIONARY POINT

TEMIRBAYEVA, M. K., Tajik State University imeni V. I. Lenin

[Abstract] The hamiltonian of perturbed motion in action-angle variables is
found for a gyrostat.   The analysis is based on work by Popa and
Aksenenkova (M. P. Popa, IZVESTIYA [AKADEMII NAUK] MOLDAVSKOY SSR:
SERIYA FIZIKO-TEKHNICHESKIKH I MATEMATICHESKIKH NAUK, No 2, 1975; I. M.
Aksenenkova, V. G. Demin, in: "Pyatyy vsesoyuznyy s"yezd po teoreticheskoy
i prikladnoy mekhanike Kazakhskoy SSR. Annotatsii dokladov" [Fifth All-Union
Congress on Theoretical and Applied Mechanics, Kazakh SSR. Abstracts of
Papers], 1981, p 24). Resonant tori and the existence of periodic motions
on them are studied on the basis of work by H. Poincaré. References 3
Russian.
[138-6610]

FLUID MECHANICS

CALCULATING ISOTHERMAL FLOW IN WAKE BEYOND INJECTION ZONE

KRUTOVA, N. M. and MITYUSHKINA, T. A.

[Abstract] An interesting method of calculating flows with injection and
flow in a wake beyond an injection area is that based on the hypothesis of
similarity of small scale turbulent structures with respect to the Reynolds
number of the turbulence. The method is suitable for gradient flows and
flows with injection and with heat exchange. The system of equations des-
cribing the flow in a turbulent boundary layer is presented and used to study
the turbulent flow in a wake beyond an injection zone in a permeable flat
plate. A comparison of experimental and calculated data was performed based
on medium speed profiles, yielding satisfactory agreement of experimental
and calculated results. Figure 1, references 7 Russian.
[124-6508]

AUTOMATING THE STUDY OF ERROR IN DISCRETE AERODYNAMIC FAIRING DESIGN

ITSKOVICH, I. I.

[Abstract] A study is made of the assignment of a set of coordinates for
numerical control of a machine tool to generate an aerodynamic shape. The
possibility is studied of automating monitoring of the coordinate error of
a gas dynamic fairing by the use of a computer. The mathematical method for
estimating the error is based on the theory of linear digital signal filtra-
tion. A study of the effectiveness of linear digital filtration was per-
formed during calculation for the production of turbine compressor blades.
The error of each internal point on the profile was estimated and coordinate
noise characteristics computed. The estimates were used to determine serious

errors in coordinates, beyond the statistical distribution. These points
were then discarded. The resolution of the digital filter was found to
be 0.0001 mm. At least 10 points should be used to get local and statistical
estimates of coordinate errors. About 100 points per minute can be computed
on a YeS-1022 computer. Figures 3, references 5 Russian.
[124-6508]

CALCULATING BOUNDARY LAYER ON PROFILE WITH LAMINAR AND TURBULENT FLOW ZONE

SOVERSHENNYY, V. D. and ALEKSIN, V. A.

[Abstract] A numerical method is applied to solve partial differential equa-
tions allowing direct determination of the influence of the hypothesis of
turbulence on the final results when laminar, transition and turbulent
flow zones are present on a profile, as well as consideration of the simul-
taneous influence of a number of factors in the problem. Calculated and
experimental data are compared. The system of equations includes equations
for discontinuity, equations of motion, energy and state. Figures 4,
references 10: 8 Russian, 2 Western.
[124-6508]

MODEL OF FRICTION BEARING HYDRODYNAMICS

CHEREBATSKIY, S. B.

[Abstract] The following model of the operation of a bearing is analyzed.
The pressure in the fluid cannot be measured. The flow of lubricant occurs
at a constant temperature. Laminar flow of fluid with full adhesion of the
fluid to the walls is studied. In the area where laminar flow is impossible
the pressure is assumed to be atmospheric. The variation of pressure as a
function of flow rate of lubricant is determined. The basic conclusions of
the article can be applied to gas bearings as well. Figures 2, references
6 Russian.
[124-6508]

FORMULA FOR VELOCITY AT VISCOUS SUBLAYER BOUNDARY

GILIMZYANOV, F. G.

[Abstract] An equation is derived which defines the velocity of turbulent flow at the boundary of a viscous sublayer. References 2 Russian.
[124-6508]

LIMITING CASE OF HYPERSONIC IDEAL GAS FLOW AROUND A THIN SHARP PROFILE

MONAKHOV, N. M. and MIGUNOV, V. V.

[Abstract] A study is made of the flow of a nonviscous, non-heat conducting gas with attached shock wave and infinite Mach number of the incident flow. An equation is presented for the pressure coefficient on the profile. The method of rarefaction waves is utilized in the study. Figures 3, references 3: 2 Russian, 1 Western.
[124-6508]

FORCES ACTING ON SPHERICAL PARTICLE IN ACOUSTIC FIELD IN VISCOUS LIQUID

GUZ', A. N., member, Ukrainian SSR Academy of Sciences and ZHUK, A. P., Institute of Mechanics, Ukrainian SSR Academy of Sciences

[Abstract] The average forces impinging from a viscous liquid on a small particle in the field of an acoustic wave are examined. The axisymmetrical problem of the interaction of a spherical particle with a plane wave is examined. The influence of viscosity on the average hydrodynamic force depends on the ratio of the density of the liquid and the particle material. Viscosity is shown to increase the average hydrodynamic force as that ratio increases for particles that are lighter than the liquid. There is a critical value of the ratio for particles that are heavier than the liquid

for which the viscosity reduces the average hydrodynamic force to the greatest extent. References 7: 6 Russian, 1 Western.
[201-6900]

PROBLEM OF REDUCTION TO "IDEAL TUBE" IN EXPERIMENTAL AERODYNAMICS

YANENKO, N. N., VOSKOBOYNIKOV, Yu. Ye. and PREOBRAZHENSKIY, N. G., Institute of Theoretical and Applied Mechanics, Siberian Department, USSR Academy of Sciences

[Abstract] A linearized statement of the problem of eliminating the spread function (reduction to "ideal tube") in measuring the amplitude of pulsations of a turbulent flow is examined. Regularization methods are used to eliminate the distorting influence of the spread function of the aerodynamic tube and to solve the problem of reduction to an "ideal tube" when investigating the distribution density of amplitude pulsations of a turbulent flow. Figures 2, references 7: 5 Russian, 2 Western.
[201-6900]

HEAT EXCHANGE OF CYLINDER EXPOSED TO TRANSVERSE FLOW OF WATER WITH PULSATING TEMPERATURE

SERGEYEVA, L. A., Institute of Thermal and Mass Exchange imeni A.V. Lykova, BSSR Academy of Sciences

[Abstract] When a fluid flows around a cylindrical body and the fluid temperature is not that of the body, the heat exchange occurring in the case of transverse flow can be described by a simple empirical equation relating the Nu to the Re and Pr numbers for the upstream side of the cylinder. However, this expression is invalid when the fluid temperature changes periodically. The periodically repeating process of thermal boundary layer formation can affect the heat exchange rate under certain conditions. In this analysis of laminar steady fluid flow around a cylinder, it is assumed that the fluid has constant properties and the fluid temperature changes periodically in a step between two values. Initially, an expression is found for the relative non-steady-state heat exchange coefficient in a process with a single temperature step change for a slender heat conducting

cylinder (disregarding the temperature gradient through the cylinder). This single step case, solved by numerical simulation, is then used to derive a more complex analytical equation for the relative heat exchange coefficient in the case of a periodic stepwise change. It is shown that in this latter case, the average heat exchange coefficient can differ by a factor of several times from that calculated using the earlier simpler formulas for steady-state solutions. The heat exchange is illustrated by graphs of the exchange coefficient as a function of the period of flow temperature pulsations. Figure 1, references 3 Russian.
[173-8225]

MECHANICS OF SOLIDS

COMPUTATIONS FOR SEGMENTED RADIAL BEARINGS

TOKAR', I.Ya., Doctor of technical sciences, SAYCHUK, I.V., candidate of technical sciences, and VISHNIVETSKIY, M.G., engineer

[Abstract] Segmented radial bearings are subject to thermal deformation significantly greater than that due to loading, which can be reduced by forced cooling of the working surface better than by oil baths that develop higher temperatures. Prognosis of working characteristics of the cooled segmented radial bearings involves computation of process non-isothermicity in the system. A method was used involving a system of equations for movement, mass and energy describing the flow of viscous imcompressible liquid in the lubricating system, which was computer solved. Basic bearing characteristics were computed and working surface temperature and heat removal data were generated. Experimental data were obtained for temperatures, pressure, friction, loading and lubricant flow that agreed with computations. Optimal parameters can then be chosen for segmented radial bearings as concerns temperature control. The maximum babbit metal values can be reduced 20-25°C for specific loads and heat extraction from the surface can be increased by an additional 5-7°C by intensified removal, lubricant channel increase and use of other materials. Figures 5, references 5 Russian. [127-12497]

KINEMATICS OF PLANE-PARALLEL MOTION OF TRANSPORT MACHINES IN CONTINUOUS SEGMENTS USING WHEELED-STEPPING PROPELLING DEVICES

SIDORENKO, S. I., graduate student

[Abstract] A case is studied of uniform, translational, plane-parallel motion in continuous segments by a wheeled-stepping transport device. At

each moment in time, the motion can be represented as the result of inter-
action of individual wheeled-stepping devices with the ground, some of
which are supporting the transport device, while the others are
advancing through the air. Equations and graphs are derived that describe
this motion. A typical device of this type has three eccentric stepping
wheels on each side, so that the device is supported by two on one
side and one on the other while the other three stepping wheels
advance. Figures 2, references 3 Russian.
[132-6508]

EXPANSION OF THICKWALL CYLINDERS AND SPHERES

MALININ, N.N., Doctor of technical sciences, professor

[Abstract] A study is made of a thickwall cylinder to determine the stress
and strain states when the specimen is loaded by internal pressure under
creep conditions. The stress is determined using the differential equation
of equilibrium of an element cut from a pipe. Curves of dimensionless
stresses are presented. Figures 3.
[132-6508]

STRENGTH COMPUTATION OF THIN WALLED SHELL BY DISCREET-CONTINUOUS MODEL

SHATAYEV, V. G. and SAMARTSEV, A. G.

[Abstract] A numerical method is suggested for determining the stress-
strain state of a reinforced shell of arbitrary cross section considering
elasticity of the ribs. The body is assumed to be divided into sections
or compartments, either of which is a set of flat panels, straight stiffen-
ing ribs and frame rib structures with finite rigidity in plane and absolute
compliance out of plane. A discrete-continuous model is used to describe
the stress-strain state, assuming a thin, zero-moment skin which accepts
only shear stress, its operation in response to perpendicular stresses being
computed considering attached strips. The rigidity characteristics
of each section are considered to be arbitrary functions of the longitudinal
coordinate. The elasticity of the ribs is found to have a significant
influence on the stress-strain state of the structure at the point of load
application. Figures 4, references 3 Russian.
[124-6508]

DESIGN OF SWEPT WING SHELL

BULATOV, S. N. and KUROCHKA, P. N.

[Abstract] A study is made of the stress-strain state of a caisson-type shell for a swept wing with a wall thickness which varies exponentially. Figures 3, references 5 Russian.
[124-6508]

OPTIMIZATION OF FIXED-MASS CYLINDRICAL SHELL UNDER EXTERNAL PRESSURE

RYABTSEV, V. A., Voronezh

[Abstract] In this article the problem of optimizing the maximum external critical pressure of a circular cylindrical shell loaded by pressure that changes along the axis of the shell is studied. The algorithm suggested for selecting the possible direction of variation cannot be reduced to the algorithm of planning the gradient of a functional in an area, since it requires correction of the vector H. The algorithm implements a directed search and can yield only locally optimal solutions. Figures 2, references 5 Russian.
[151-6508]

STABILITY OF NONLINEAR FORCED OSCILLATIONS OF SMOOTH CYLINDRICAL SHELLS OF RECTANGULAR PLANFORM

GRIGORENKO, Ya. M., GULYAYEV, V. I., DEKHTYARYUK, Ye. S. and CHEMLAYEV, V. V., Kiev

[Abstract] A study is made of the steady oscillation of thin smooth cylindrical shells of rectangular planform compressed along the generatrix by uniform forces.   The method used is based on representation of the

calculation model of the shell as a system with one degree of freedom. Stable oscillations of shells under uniformly distributed surface loads exchanged according to a harmonic rule are studied. The Bubnov-Galerkin method reduces the problem to consruction of periodic solutions of ordinary differential equations. Figures 4, references 6 Russian.
[151-6508]

DIFRACTION OF ELASTIC WAVES ON SEPARATIONS IN SPHERICAL MULTILAYER SHELLS

LOBANOV, Ye. V., Moscow

[Abstract] A continuous analog of the theory of multilayer shells and plates is used as a model to describe the propagation of waves in a shell consisting of small layers. The problem of radiation of elastic waves by a crack is studied. It is shown that waves diffracted on the crack satisfy a condition described by equations developed in the article on a rib and conditions of radiation as kr approaches infinity. An algorithm is presented for determination of the location, depth and size of a defect based on a steady echo signal. Figures 4, references 6: 3 Russian, 3 Western.
[151-6508]

WORK OF AXIAL BEARING UNDER DYNAMIC LOADING

ZARETSKIY, Ye. I., SEREZHKINA, L. P. and USACHEV, I. D., candidates of technical sciences

[Abstract] Studies of the operation of thrust bearings under transient conditions were performed on a full-scale test-stand installation (thrust disk diameter 580 mm) with bearings having reduced load-bearing capacity. Thermocouples were installed at distances of 4 mm from the load-bearing surface. At loading rates exceeding 100 tf/s, the temperature measured by the thermocouple lags far behind the actual temperature at the friction surface. Triple dynamic loading of the bearing by identical forces at equal time intervals was modeled on the test stand. The results of the experiments indicated that under dynamic operating conditions there is no unambiguous variation between the temperature of the bearing and the load at any moment in time. Bearing temperature therefore cannot be considered as an on-line indicator of thrust bearing reliability. Figures 5, references 2 Russian.
[128-6508]

LOAD-BEARING CAPACITY OF FIBERGLASS PLASTIC BLADE ON AXIAL BLOWER

ZAYTSEV, G. P., SILANT'YEV, S. A., BUKHIN, V. Ye., ZHUKOV, N. I. and MEL'NIKOV, V. P., Moscow Aviation Technology Institute

[Abstract] Fiberglass plastic blades are replacing metal in axial blowers because of better technological properties, freedom from corrosion and better damping characteristics, as well as lower weight than metal blades. In this article, the authors discuss the load-bearing capacity of a blade of fiberglass plastic in the VO-1 blower. This blade is made of satin-weave ASTT-S$_2$ fiberglass with EF33-301 epoxy binder. The blade is produced by direct molding, and has precision geometric dimensions and good surface finish. Tests were done under both momentary and cyclic loading, with measurements of characteristics of elasticity, strength and fatigue of the blade material, and the results were used to calculate the strength reserve in the most heavily loaded cross section with momentary static application of operating loads, and to calculate the service life of blades under cyclic loading. To determine the possibility of resonance occurring at the working speed of the blower, the natural frequencies of blade vibrations were theoretically calculated and experimentally measured. The results of the studies show a good outlook for effective use of fiberglass plastic blades in blowers. Figures 4, table 1, references 5 Russian.
[137-6610]

END

END OF
FICHE

DATE FILMED

24 July 1984